The Astronomical Journal, 153:238 (8pp), 2017 May https://doi.org/10.3847/1538-3881/aa6c2a

Cyclic Period Oscillation of the Eclipsing Dwarf Nova DV UMa

Z.-T Han[1,2,3], S.-B Qian[1,2,3], Voloshina Irina[4], and L.-Y Zhu[1,2,3]
[1] Yunnan Observatories, Chinese Academy of Sciences (CAS), P.O. Box 110, 650216 Kunming, China; zhongtaohan@ynao.ac.cn
[2] Key Laboratory of the Structure and Evolution of Celestial Objects, Chinese Academy of Sciences, P.O. Box 110, 650216 Kunming, China
[3] University of Chinese Academy of Sciences, Yuquan Road 19#, Sijingshang Block, 100049 Beijing, China
[4] Sternberg Astronomical Institute, Moscow State University, Universitetskij prospect 13, Moscow 119992, Russia
Received 2017 February 20; revised 2017 March 26; accepted 2017 April 4; published 2017 May 3

Abstract

DV UMa is an eclipsing dwarf nova with an orbital period of ∼2.06 hr, which lies just at the bottom edge of the period gap. To detect its orbital period changes, we present 12 new mid-eclipse times by using our CCD photometric data and archival data. The latest version of the *O–C* diagram, combined with the published mid-eclipse times in quiescence, and spanning ∼30 years, was obtained and analyzed. The best fit to those available eclipse timings shows that the orbital period of DV UMa is undergoing a cyclic oscillation with a period of 17.58(±0.52) years and an amplitude of 71.1(±6.7) s. The periodic variation most likely arises from the light-travel-time effect via the presence of a circumbinary object, because the required energy to drive the Applegate mechanism is too high in this system. The mass of the unseen companion was derived as $M_3 \sin i' = 0.025(\pm 0.004)\, M_\odot$. If the third body is in the orbital plane (i.e., $i' = i = 82.^\circ 9$) of the eclipsing pair, this would indicate it is a brown dwarf. This hypothetical brown dwarf is orbiting its host star at a separation of ∼8.6 au in an eccentric orbit ($e = 0.44$).

Key words: binaries: close – binaries: eclipsing – stars: dwarf novae – stars: individual (DV UMa)

1. Introduction

Cataclysmic variables (CVs) are short-period binaries containing a white dwarf and a low-mass donor star that is transferring material to the white dwarf via an accretion disc (Warner 1995). The structure of CVs allows for precise timing measurements, because the components have large differences in radius and luminosity (e.g., Parsons et al. 2010). The timing measurements offer important clues concerning the long-term evolution of orbital periods and the existence of circumbinary substellar objects. By analyzing the observed–calculated (*O–C*) curve of these systems, the orbital period and its rate of change can be measured. The secular change of the *O–C* curve can provide key information on the evolution of CVs (Qian et al. 2015). Moreover, if there is a third body orbiting the close binary system, it will cause a small wobble, cyclically, in the timing of eclipses. More specifically, if a third body exists, then the binary system and companion revolve around their common barycenter. While the system is on the near side of the larger orbit, the observed times of eclipses will be detected sooner than those on the far side. This will lead to alternating variations of the observed eclipse timings, which is often referred to as the light-travel-time (LTT) effect. The LTT shows a periodic variation in the *O–C* diagram. The timing method has recently been used to detect possible extrasolar planets around CVs such as V2051 Oph (Qian et al. 2015), Z Cha (Dai et al. 2009), OY Car (Han et al. 2015), and V893 Sco (Bruch 2014).

As a member of the dwarf nova-type CVs, DV UMa was first discovered as an ultraviolet excess object by Usher et al. (1982). Subsequently, this star was identified as a candidate dwarf nova based on the observed outburst phenomena and the Hα emission line in optical spectra (Usher et al. 1983). Howell et al. (1987) presented photometric observations that showed large brightness changes on a shorter timescale. Further photometric observations by Howell et al. (1988) revealed that DV UMa is an eclipsing system, and its orbital period was estimated as 0.08579(1) days. The system parameters were derived by Howell & Blanton (1993) using photometric analysis and by Szkody & Howell (1993) using time-resolved spectroscopy. Subsequently, these parameters have been improved to give higher precision (e.g., Patterson et al. 2000; Feline et al. 2004; Savoury et al. 2011). However, we still know little about its evolution and period changes. Although mid-eclipse times of DV UMa have been published in the literature and the orbital ephemeris has been updated by several authors, no sign of orbital period change was found (Howell et al. 1988; Patterson et al. 2000; Nogami et al. 2001; Feline et al. 2004). In this paper, we present new CCD photometric observations of DV UMa and detect a cyclic variation in the *O–C* diagram. We end with a discussion on the presence of a substellar companion.

2. Observations and Data Preparation

New CCD photometric observations of DV UMa were carried out by using three different telescopes. Beginning on 2009 November 12, this star was continuously monitored with the 2.4 m telescope at the Lijiang observational station of Yunnan Observatories (YNAO). To collect more data for this binary, an observation was made on 2016 March 29 with an Andor DW436 1K CCD camera mounted on the 85 cm reflecting telescope at the XingLong station of the National Astronomical Observatory and another observation made on 2017 January 23 with an Andor DW936 2K CCD camera attached to the 1.0 m reflecting telescope at YNAO. During the observations, no filters were used in order to improve the time resolution. All observed CCD images were analyzed by applying the aperture photometry package of IRAF. Differential photometry was performed with a nearby non-variable comparison star. Four eclipse profiles observed with the 2.4 m and 1.0 m are displayed in Figure 1. To measure the mid-eclipse times ($T_{\rm mid}$) of the white dwarf, we use the method described by Wood et al. (1985). First, the mid-ingress ($T_{\rm i}$) and

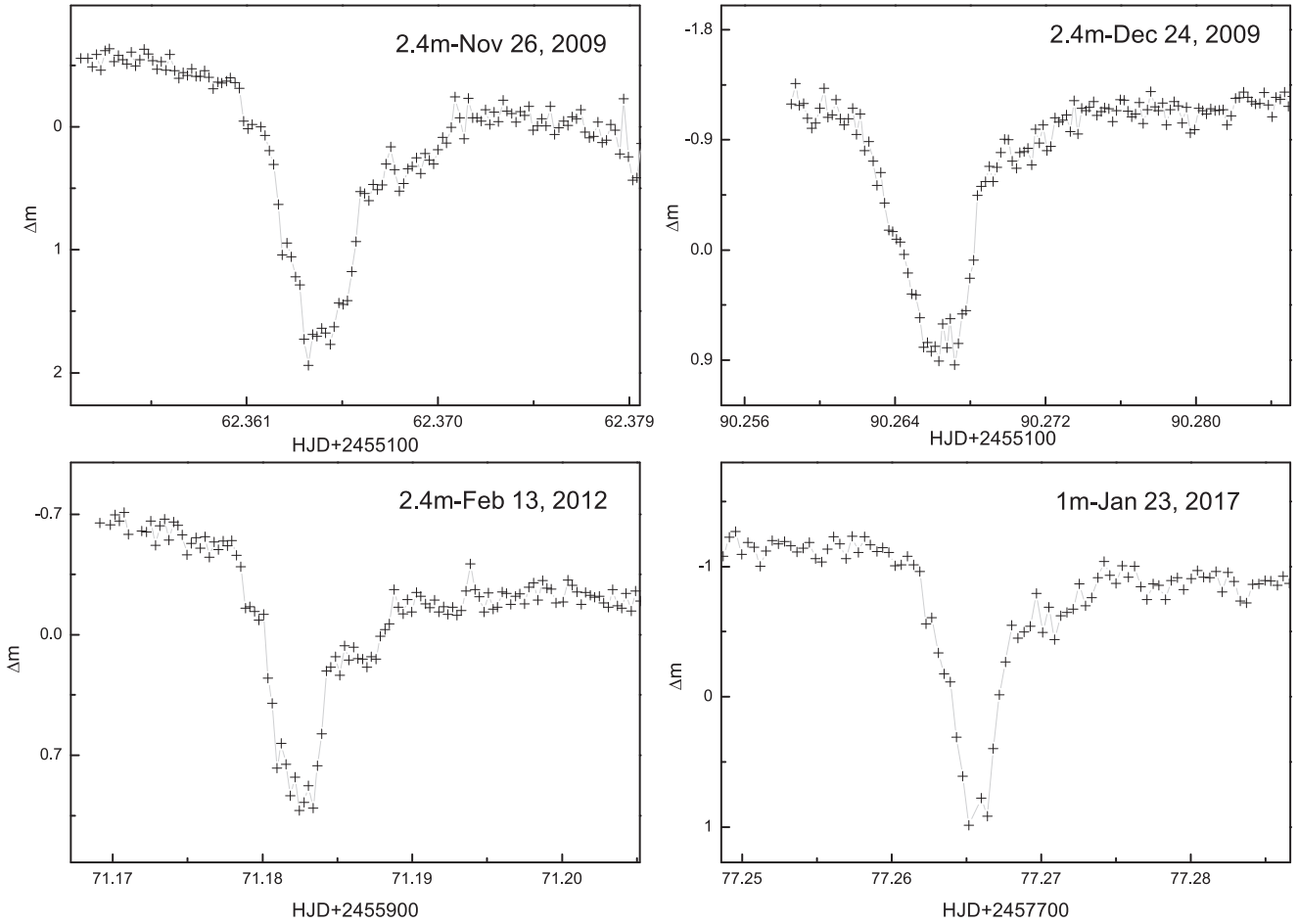

Figure 1. Four eclipse profiles of DV UMa in quiescence obtained at YNAO using the 1.0 and 2.4 m telescopes.

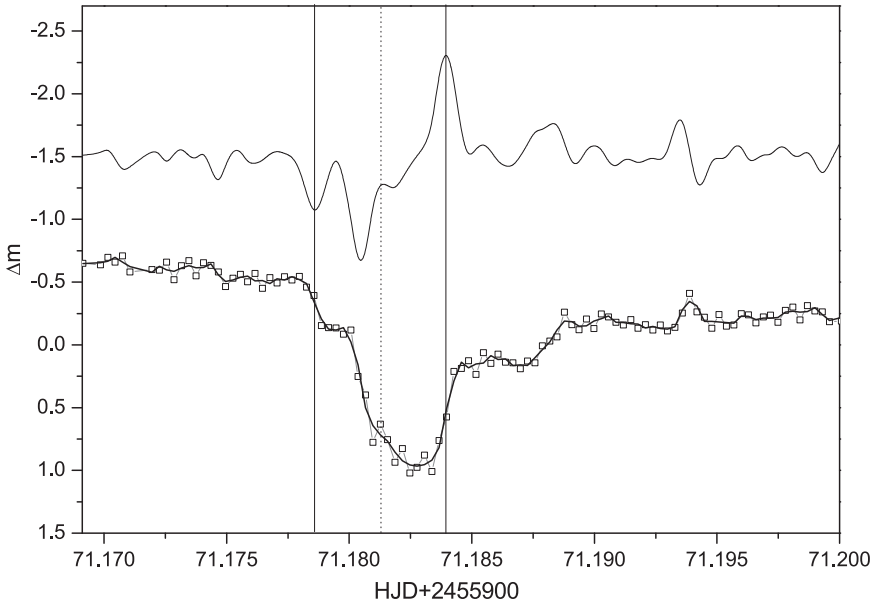

Figure 2. A sample of determining mid-egress times. The boxes denote the observed light curve, and the solid curve is the corresponding smoothed light curve. The derivative of the smoothed curve with a spline fit is plotted in the upper part of the diagram. The two vertical solid lines refer to the mid-ingress and mid-egress times of the white dwarf, while the dashed vertical line refers to the mid-eclipse times.

mid-egress times (T_e) of the white dwarf were determined by locating the maximum and minimum values of the derivative of the light curves. Then, the mid-eclipse times were derived by using $T_{mid} = (T_i + T_e)/2$. The procedure of measuring T_{mid} is illustrated in Figure 2. It is important to note that only data during quiescence were used to determine the mid-eclipse

Table 1
All Mid-eclipse Times of DV UMa

Min.(HJD)	*E*	*O–C*	Errors	State	Telescopes	References
2446854.7485	1	−0.00015	0.00050	quiescence	⋯	(1)
2446854.8339	2	−0.00060	0.00050	quiescence	⋯	(1)
2446854.9195	3	−0.00086	0.00050	quiescence	⋯	(1)
2446855.6944	12	0.00137	0.00050	quiescence	⋯	(1)
2446855.7798	13	0.00092	0.00050	quiescence	⋯	(1)
2446855.8660	14	0.00126	0.00050	quiescence	⋯	(1)
2446855.9517	15	0.00111	0.00050	quiescence	⋯	(1)
2446856.4646	21	−0.0011	0.00050	quiescence	⋯	(1)
2446856.5503	22	−0.00126	0.00050	quiescence	⋯	(1)
2446856.6370	23	−0.00041	0.00050	quiescence	⋯	(1)
2446857.4963	33	0.00036	0.00050	quiescence	⋯	(1)
2446857.5815	34	−0.00029	0.00050	quiescence	⋯	(1)
2449775.9693	34027	−0.00050	0.00020	outburst	⋯	(2)
2449776.0552	34028	−0.00040	0.00020	outburst	⋯	(2)
2449776.1409	34029	−0.00060	0.00020	outburst	⋯	(2)
2449776.2269	34030	−0.00050	0.00020	outburst	⋯	(2)
2449778.5451	34057	−0.00030	0.00020	quiescence	⋯	(2)
2449778.6312	34058	0.00000	0.00020	quiescence	⋯	(2)
2450548.3860	43024	0.00020	0.00010	outburst	⋯	(3)
2450548.4727	43025	0.00104	0.00010	outburst	⋯	(3)
2450548.5570	43026	−0.00051	0.00010	outburst	⋯	(3)
2450548.6440	43027	0.000639	0.00010	outburst	⋯	(3)
2450548.7310	43028	0.00179	0.00010	outburst	⋯	(3)
2450548.8144	43029	−0.00067	0.00010	outburst	⋯	(3)
2450549.0730	43032	0.00040	0.00020	outburst	⋯	(2)
2450549.1578	43033	−0.00070	0.00020	outburst	⋯	(2)
2450549.4180	43036	0.00197	0.00010	outburst	⋯	(3)
2450549.5032	43037	0.00131	0.00010	outburst	⋯	(3)
2450550.3609	43047	0.00049	0.00010	outburst	⋯	(3)
2450550.4463	43048	0.00003	0.00010	outburst	⋯	(3)
2450551.3894	43059	−0.00124	0.00010	outburst	⋯	(3)
2450551.4754	43060	−0.00110	0.00010	outburst	⋯	(3)
2450551.7351	43063	0.00105	0.00010	outburst	⋯	(3)
2450551.8202	43064	0.00029	0.00010	outburst	⋯	(3)
2450551.9916	43066	0.00000	0.00020	outburst	⋯	(2)
2450552.0776	43067	0.00010	0.00020	outburst	⋯	(2)
2450552.1630	43068	−0.00030	0.00020	outburst	⋯	(2)
2450552.4214	43071	0.00050	0.00020	outburst	⋯	(2)
2450552.5927	43073	0.00012	0.00010	outburst	⋯	(3)
2450553.3643	43082	−0.00095	0.00010	outburst	⋯	(3)
2450553.4512	43083	0.00009	0.00010	outburst	⋯	(3)
2450553.6234	43085	0.00059	0.00010	outburst	⋯	(3)
2450553.7093	43086	0.00064	0.00010	outburst	⋯	(3)
2450554.3945	43094	−0.00099	0.00010	outburst	⋯	(3)
2450554.4799	43095	−0.00144	0.00010	outburst	⋯	(3)
2450554.5672	43096	0.00001	0.00010	outburst	⋯	(3)
2450554.6530	43097	−0.00004	0.00010	outburst	⋯	(3)
2450554.7393	43098	0.00040	0.00010	outburst	⋯	(3)
2450554.8248	43099	0.00005	0.00010	outburst	⋯	(3)
2450555.3394	43105	−0.00046	0.00010	outburst	⋯	(3)
2450555.4252	43106	−0.00052	0.00010	outburst	⋯	(3)
2450555.4267	43106	0.00100	0.00020	outburst	⋯	(2)
2450557.6584	43132	0.00051	0.00010	outburst	⋯	(3)
2450557.7441	43133	0.00036	0.00010	outburst	⋯	(3)
2450557.8295	43134	−0.00009	0.00010	outburst	⋯	(3)
2450558.3446	43140	−0.00011	0.00010	outburst	⋯	(3)
2450560.6630	43167	0.00027	0.00010	outburst	⋯	(3)
2450560.7491	43168	0.00052	0.00010	outburst	⋯	(3)
2450561.6935	43179	0.00054	0.00010	outburst	⋯	(3)
2450561.7798	43180	0.00099	0.00010	outburst	⋯	(3)
2450562.3794	43187	−0.00040	0.00020	outburst	⋯	(2)
2450562.4654	43188	−0.00020	0.00020	outburst	⋯	(2)
2450562.6369	43190	−0.00044	0.00010	outburst	⋯	(3)
2450562.7227	43191	−0.00049	0.00010	outburst	⋯	(3)

Table 1
(Continued)

Min.(HJD)	E	$O-C$	Errors	State	Telescopes	References
2450563.0667	43195	0.00010	0.00020	outburst	⋯	(2)
2450563.6678	43202	0.00023	0.00010	outburst	⋯	(3)
2450564.0123	43206	0.00130	0.00020	outburst	⋯	(2)
2450564.0967	43207	−0.00010	0.00020	outburst	⋯	(2)
2450564.6984	43214	0.00060	0.00010	outburst	⋯	(3)
2450565.6430	43225	0.00082	0.00010	outburst	⋯	(3)
2450565.7284	43226	0.00037	0.00010	outburst	⋯	(3)
2450565.8145	43227	0.00062	0.00010	quiescence	⋯	(3)
2450566.6731	43237	0.00069	0.00010	quiescence	⋯	(3)
2450566.8448	43239	0.00068	0.00010	quiescence	⋯	(3)
2450567.7888	43250	0.00031	0.00010	quiescence	⋯	(3)
2450949.6625	47698	0.00156	0.00010	quiescence	⋯	(3)
2451164.8951	50205	0.00165	0.00010	quiescence	⋯	(3)
2451211.8562	50752	0.00137	0.00010	quiescence	⋯	(3)
2451212.8861	50764	0.00104	0.00010	quiescence	⋯	(3)
2451523.4147	54381	0.00072	0.00010	outburst	⋯	(3)
2451523.5007	54382	0.00087	0.00010	outburst	⋯	(3)
2451523.5862	54383	0.00052	0.00010	outburst	⋯	(3)
2451523.9299	54387	0.00081	0.00010	outburst	⋯	(3)
2451524.0160	54388	0.00106	0.00010	outburst	⋯	(3)
2451526.5051	54417	0.00043	0.00010	outburst	⋯	(3)
2451526.8496	54421	0.00152	0.00010	outburst	⋯	(3)
2451526.9350	54422	0.00107	0.00010	outburst	⋯	(3)
2451531.4854	54475	0.00128	0.00010	outburst	⋯	(3)
2451531.7424	54478	0.00072	0.00010	outburst	⋯	(3)
2451531.8282	54479	0.00067	0.00010	outburst	⋯	(3)
2451531.9140	54480	0.00061	0.00010	outburst	⋯	(3)
2451532.6008	54488	0.00059	0.00010	outburst	⋯	(3)
2451532.6867	54489	0.00064	0.00010	outburst	⋯	(3)
2451578.9620	55028	0.00138	0.00010	quiescence	⋯	(3)
2451579.0480	55029	0.00153	0.00010	quiescence	⋯	(3)
2451584.7144	55095	0.00166	0.00010	quiescence	⋯	(3)
2451584.7999	55096	0.00130	0.00010	quiescence	⋯	(3)
2452780.46923	69023	0.00123	0.00004	quiescence	⋯	(4)
2452782.44381	69046	0.00120	0.00004	quiescence	⋯	(4)
2452783.47405	69058	0.00121	0.00004	quiescence	⋯	(4)
2455148.36951	96604	0.00048	0.00010	quiescence	2.4 m	(6)
2455162.36340	96767	0.00039	0.00010	quiescence	2.4 m	(6)
2455189.32165	97081	0.00092	0.00050	quiescence	⋯	(5)
2455190.26572	97092	0.00061	0.00010	quiescence	2.4 m	(6)
2455971.18127	106188	0.00075	0.00005	quiescence	2.4 m	(6)
2456711.66042	114813	0.00108	0.00070	quiescence	⋯	(5)
2456712.77675	114826	0.00133	0.00070	quiescence	⋯	(5)
2456714.83747	114850	0.00158	0.00070	quiescence	⋯	(5)
2457465.27595	123591	0.00234	0.00010	quiescence	2.4 m	(6)
2457466.30594	123603	0.00210	0.00010	quiescence	2.4 m	(6)
2457477.12345	123729	0.00218	0.00010	quiescence	85 cm	(6)
2457777.26444	127225	0.00242	0.00010	quiescence	1.0 m	(6)

References. (1) Howell et al. (1988), (2) Nogami et al. (2001), (3) Patterson et al. (2000), (4) Feline et al. (2004), (5) AAVSO data, (6) Our observations.

times, because the system in outburst is dominated by the accretion disc, and the T_i and T_e of the white dwarf are not clearly identified in the derivative curve. However, during quiescence, the ingress and egress times of the white dwarf are stable features. As shown in Figure 2, the white dwarf and bright-spot ingress and egress are both clear and distinct. With our data, eight mid-eclipse times were obtained. The errors are the standard errors in measuring mid-eclipse times, and they depend on the time resolution and signal-to-noise ratio during observations. Apart from our data, four mid-eclipse times during quiescence were also determined with the observations from the American Association of Variable Star Observers (AAVSO). By checking the AAVSO database, we find that their observations contain many eclipsing light curves. Moreover, the long-term AAVSO data will help to confirm whether this star is in outburst or not. These new mid-eclipse times and their errors are listed in Table 1.

Mid-eclipse times of DV UMa have also been published in the literature by several previous authors. Howell et al. (1988) first reported twelve mid-eclipse times and an orbital ephemeris. Later, Patterson et al. (2000) updated the orbital ephemeris by adding twelve mid-eclipse times. After just one year, the ephemeris was revised again by Nogami et al. (2001). A recent version of the orbital ephemeris was determined by

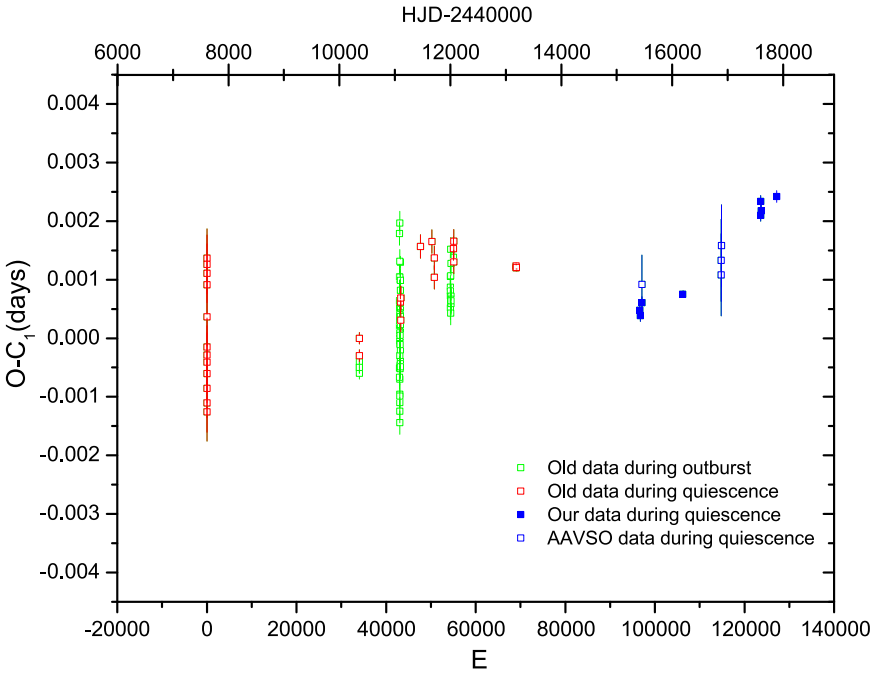

Figure 3. Latest *O–C* diagram of DV UMa, using new mid-eclipse times together with all published data. New eclipse timings in quiescence are denoted by the blue boxes (open and solid). Those data obtained from the literature can be divided into two groups: during outburst (green boxes) and during quiescence (red boxes).

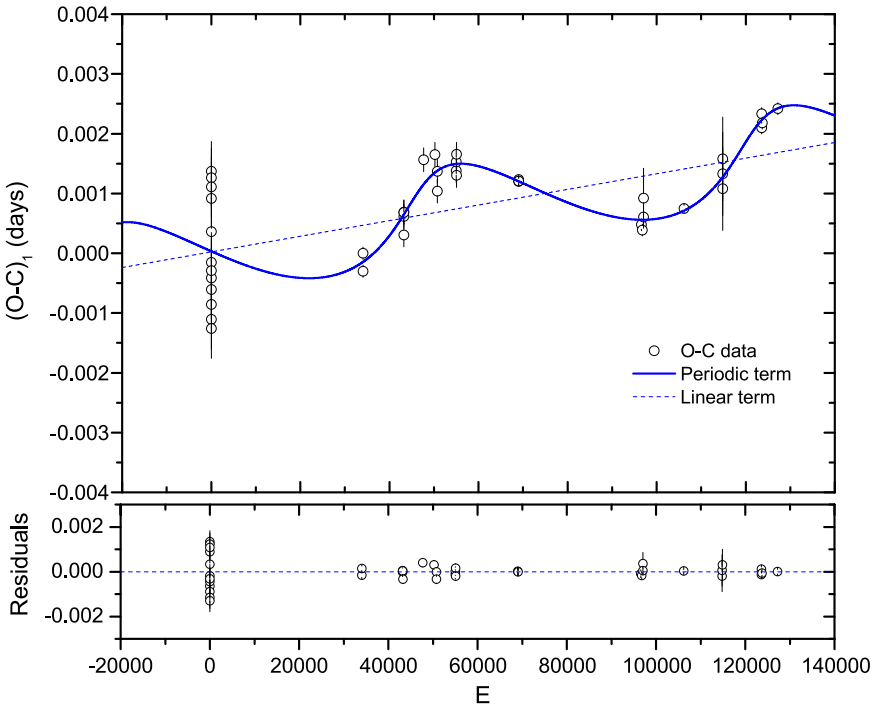

Figure 4. *O–C* diagram of DV UMa constructed with a linear plus LTT ephemeris. The black open circles refer to the data obtained in quiescence. The blue solid line in the upper panel represents the best-fit model. The lower panel displays the fit residuals from the complete ephemeris.

Feline et al. (2004). However, not all published data are suitable for the period analyses. For instance, some mid-eclipse times during outbursts should be excluded. Based on the observations of the outbursts reported by Patterson et al. (2000) and Nogami et al. (2001), the mid-eclipse times during outbursts can be separated from these historical data. These data and related information are also given in Table 1. The linear ephemeris presented by Nogami et al. (2001) is used to compute the *O–C* values of all mid-eclipse times, which are plotted in Figure 3.

3. Eclipse Timing Variation and Analysis

The orbital period of DV UMa was investigated by previous authors, but no sign of any period change was found. Based on the discussion in Section 2, only the mid-eclipse times in

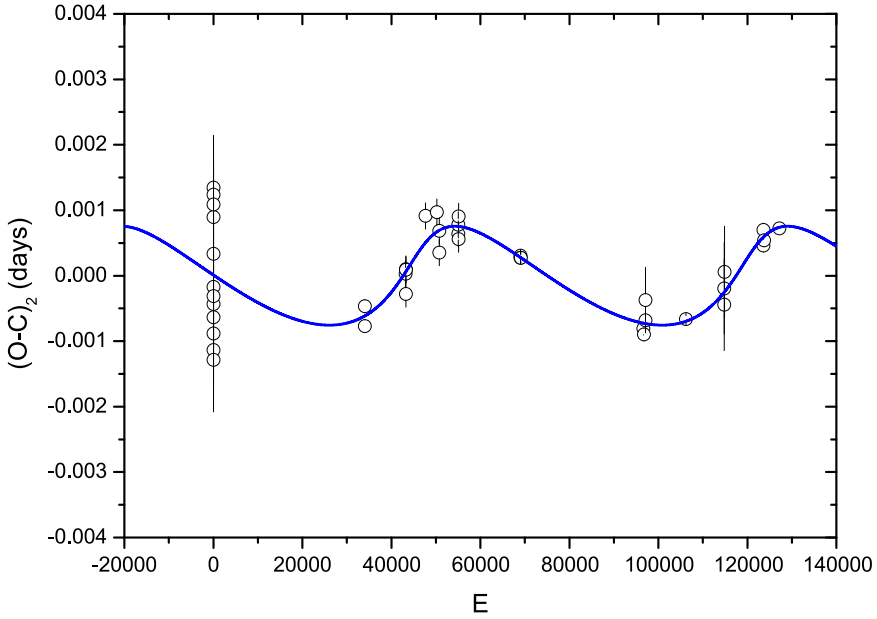

Figure 5. LTT orbit of a potential circumbinary companion extracted from the upper panel of Figure 4. As shown, the cyclic oscillation can be seen clearly.

quiescence are used for the present analysis. The updated O–C diagram is shown in Figure 4. We represent the O–C curve by a linear least-squares fit. However, the linear ephemeris cannot sufficiently represent all observed timings, and its residuals seem to show an apparent periodic oscillation. In general, the LTT via the presence of a circumbinary companion can be considered to be a possible cause of this oscillation (Irwin 1952). Therefore, the best-fit model for the O–C diagram may be represented as

$$\begin{aligned}(O\text{–}C)_1 &= \Delta T_0 + \Delta P_0 E + K\left[(1-e^2)\right.\\ &\quad\left.\times\frac{\sin(\nu+\omega)}{1+e\cos\nu}+e\sin\omega\right]\\ &= \Delta T_0 + \Delta P_0 E\\ &\quad + K\left[\sqrt{1-e^2}\sin E^*\cos\omega+\cos E^*\sin\omega\right],\end{aligned}\quad (1)$$

where ΔT_0 and ΔP_0 are the revised epoch and period, ν is the true anomaly, E^* is the eccentric anomaly, e is the orbital eccentricity, and $K = a_{12}\sin i'/c$ is the semi-amplitude of the LTT. To solve Equation (1), we used the two correlations:

$$N = E^* - e\sin E^*, \quad (2)$$

and

$$N = \frac{2\pi}{P_3}(t-T). \quad (3)$$

N is the mean anomaly and t is the time of light minimum. In the process of fitting, the weighted least-squares method was used, and the different weights were assigned to the different errors: weights 1, 5, 10, and 40 correspond to errors 0.0005 days, 0.0002 days, 0.0001 days, and 0.00005 days, respectively. All parameters and final results are summarized in Table 2. The parameter errors are computed from the best-fit covariance matrix. The residual sum of squares is ~0.00001, indicating a very good fit.

Table 2
Orbital Parameters of the Circumbinary Brown Dwarf Companion

Parameters	Values
Revised epoch, ΔT_0 (days)	$+2.28(\pm1.46)\times10^{-5}$
Revised period, ΔP_0 (days)	$+1.31(\pm0.16)\times10^{-8}$
Eccentricity, e	$0.44(\pm0.17)$
Longitude of the periastron passage, ω (deg)	$26.11(\pm21.55)$
Periastron passage, T (years)	$2444390.5(\pm424.5)$
The semi-amplitude, K (days)	$0.000822(\pm0.000077)$
Orbital period, P_3 (years)	$17.58(\pm0.52)$
Projected semimajor axis, $a_{12}\sin i'$ (au)	$0.143(\pm0.013)$
Mass function, $f(m)$ ($M_\odot$)	$9.36(\pm2.61)\times10^{-6}$
Mass of the third companion, $M_3\sin i'$ ($M_\odot$)	$0.025(\pm0.004)$
Orbital separation, d_3 (au, $i'=90°$)	$8.6(\pm1.6)$

Our results show that the orbital period of DV UMa has a cyclic variation with an amplitude of ~71.1(±6.7) s and a period of ~17.58(±0.52) years. In the upper panel of Figure 4, the dashed line denotes the linear-ephemeris revisions on the initial epoch and the orbital period. The blue solid line represents the combination of the linear ephemeris and the periodic change. The lower panel shows the residuals from the best-fit model. In order to display the periodic oscillation clearly, the $(O$–$C)_2$ values (by removing the linear ephemeris) are plotted in Figure 5.

4. Discussions and Conclusions

In this paper, we detected and analyzed of the periodic variation in the orbital period of DV UMa. Cyclic period oscillations in close binaries containing at least one cool star can be explained by a solar-type magnetic activity cycle in the late-type component (Applegate 1992). However, the Applegate mechanism may not work here, because the donor in DV UMa is a fully convective main sequence star with mass $M_2 = 0.196(\pm0.005)\,M_\odot$ (Savoury et al. 2011). Moreover, the required energies to produce the observed change were computed using the same method as proposed by Brinkworth et al. (2006). The result indicates that the required minimum

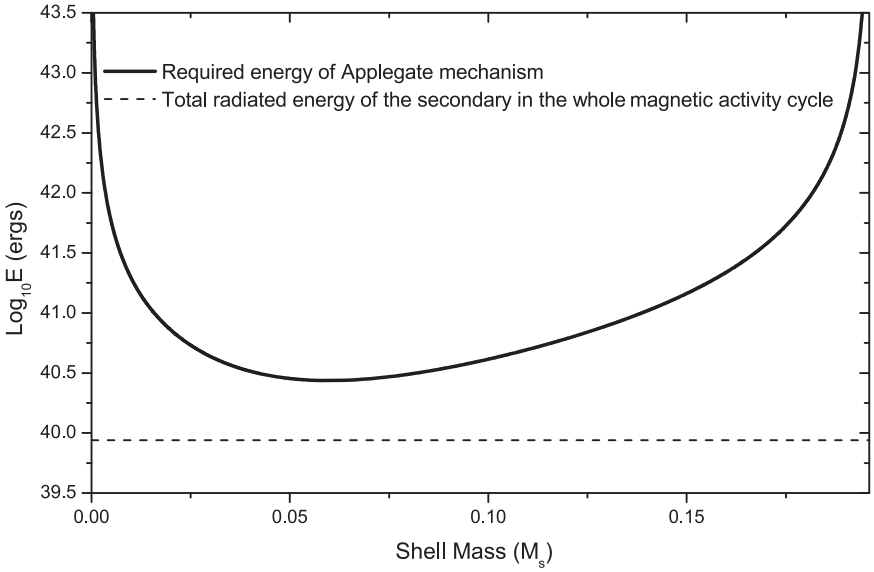

Figure 6. The solid line shows the energy required to affect the observed cyclic change in DV UMa by using the Applegate mechanism. M_s refers to the assumed shell mass of the secondary star. The dashed line represents the total energy that radiates from the donor in a whole cycle.

energy is much larger than the total energy radiated from the secondary star in a whole cycle (see Figure 6). Combining the parameters ($M_1 = 1.098\,M_\odot$, $M_2 = 0.196\,M_\odot$) presented by Savoury et al. (2011) with *Kepler*'s third law, we derived the orbital separation as $a = 0.89\,R_\odot$. Applying $T_2 = 3170\,K$ for the donor of $\sim$0.196 $M_\odot$, its luminosity can be estimated as $L_2 = (\frac{R_2}{R_\odot})^2(\frac{T_2}{T_\odot})^4 L_\odot$. Furthermore, the Applegate mechanism has been studied in depth by Völschow et al. (2016), and an improved Applegate model also has been explored. They concluded that an ideal Applegate post-common-envelope binary (PCEB) should consist of a very close orbit ($\sim$0.5 $R_\odot$) and a secondary star of $\sim$0.5 $M_\odot$. The Applegate mechanism is more feasible for a much larger donor mass than is presented here. Clearly, DV UMa cannot satisfy any of those conditions. Therefore, we suggest that the Applegate mechanism may not be responsible for this cyclic change. The most likely interpretation of the period oscillation is the LTT via the presence of an unseen companion. However, this conclusion dose not deny the presence of magnetic activity in the secondary star. On the contrary, this only implies that the magnetic activity is not the dominant mechanism here, because it cannot provide enough energy to produce the observed period variation.

The parameters of the best-fit model (see Table 2), coupled with the absolute parameters determined by Savoury et al. 2011, give mass function and mass of the tertiary companion $f(m) = 9.36(\pm2.61) \times 10^{-6}\,M_\odot$ and $M_3 \sin i' = 0.025(\pm0.004)\,M_\odot$, respectively. Assuming a random distribution of orbital plane inclinations, when $i' \geqslant 20.^\circ9$, the mass corresponds to $0.025 \leqslant M_3 \leqslant 0.07\,M_\odot$, which would match to a brown dwarf. However, the circumbinary companions are expected to be coplanar to the orbital plane of the eclipsing pair (Bonnell & Bate 1994). So, if the third body orbiting DV UMa is on a coplanar orbit (i.e., $i' = i = 82.^\circ9$), the mass is derived as $M_3 = 0.0252\,M_\odot$, and so it would be a brown dwarf. The orbital radius d_3 of the tertiary companion is $\sim$8.6($\pm$1.6) au (when $i' = 90^\circ$).

So far, only a few brown dwarfs orbiting single white dwarfs were discovered by several previous authors (e.g., Becklin & Zuckerman 1988; Farihi & Christopher 2004; Dobbie et al. 2005; Burleigh et al. 2006; Maxted et al. 2006). But in comparison with single white dwarfs, the brown dwarfs around the white dwarf binaries are more rare. Recently, only two white dwarf binaries were reported containing brown dwarf companions, i.e., V471 Tau (Guinan & Ribas 2001) and SDSS J143547 (Qian et al. 2016). Also note that the brown dwarf companion in V471 Tau was excluded by Hardy et al. (2015), but a new study agrees with the presence of a brown dwarf companion (Vaccaro et al. 2015). Moreover, some possible planets orbiting the eclipsing CVs or pre-CVs were also presented, such as V893 Sco (Bruch 2014), V2051 Oph (Qian et al. 2015), OY Car (Han et al. 2015), DP Leo (Qian et al. 2010; Beuermann et al. 2011), HU Aqr (Qian et al. 2011; Goździewski et al. 2015), UZ For (Dai et al. 2010; Potter et al. 2011), and NN Ser (Marsh et al. 2014). These discoveries suggest that the PCEBs may be one of the most common host stars. The origins of substellar objects are very complex: they may have existed before the common-envelope (CE) event (first generation; e.g., Qian et al. 2016), or they may be second generation planets (or brown dwarfs) formed during the CE phase (e.g., Völschow et al. 2014). If they are first generation companions, their masses might be increased by accreting a large amount of material during the CE stage, and more massive planets could become brown dwarf companions. But it is difficult to distinguish between these two types of substellar populations at the present. The discovery of a potential brown dwarf orbiting DV UMa may shed new light on our understanding of the origin and evolution of the circumbinary substellar objects. As yet, however, the data coverage on DV UMa is less than two cycles of the cyclic change. Further observations are critically required to ascertain whether the observed oscillation is strictly periodic, or only quasi-periodic.

This work is supported by the Chinese Natural Science Foundation (Grant Nos. 11325315, 11611530685, 11573063, and 11133007), the Strategic Priority Research Program "The Emergence of Cosmological Structure" of the Chinese Academy of Sciences (Grant Nos. XDB09010202), and the Science

Foundation of Yunnan Province (Grant Nos. 2012HC011). This study is supported by the Russian Foundation for Basic Research (project Nos. 17-52-53200). New CCD photometric observations of DV UMa were obtained with the 1 m and the 2.4 m telescopes at the Yunnan Observatories, the 85 cm telescope in Xinglong Observation base in China. We thank the numerous observers worldwide who contributed many observations of DV UMa to the AAVSO database. Finally, we thank the referee for an insightful report that has significantly improved the paper.

References

Applegate, J. H. 1992, ApJ, 385, 621
Becklin, E. F., & Zuckerman, B. 1988, Natur, 336, 656
Beuermann, K., Buhlmann, J., Diese, J., et al. 2011, A&A, 526, A53
Bonnell, I. A., & Bate, M. R. 1994, MNRAS, 269, L45
Brinkworth, C. S., Marsh, T. R., Dhillon, V. S., & Knigge, C. 2006, MNRAS, 365, 287
Bruch, A. 2014, A&A, 566, 101
Burleigh, M. R., Hogan, E., Dobbie, P. D., et al. 2006, MNRAS, 373, L55
Dai, Z. B., Qian, S. B., & Fernándes Lajús, E. 2009, ApJ, 703, 109
Dai, Z.-B., Qian, S.-B., Fernández Lajús, E., & Baume, G. L. 2010, MNRAS, 409, 1195
Dobbie, P. D., Burleigh, M. R., Levan, A. J., et al. 2005, MNRAS, 357, 1049
Farihi, J., & Christopher, M. 2004, AJ, 128, 1868
Feline, W., Dhillon, V., Marsh, T., & Brinkworth, C. 2004, MNRAS, 355, 1
Goździewski, K., Słowikowska, A., Dimitrov, D., et al. 2015, MNRAS, 448, 1118
Guinan, E. F., & Ribas, I. 2001, ApJL, 546, L43
Han, Z.-T., Qian, S. B., Fernándes Lajús, E., et al. 2015, NewA, 34, 1
Hardy, A., Schreiber, M. R., Parsons, S. G., et al. 2015, ApJL, 800, L24
Howell, S. B., & Blanton, S. A. 1993, AJ, 106, 311
Howell, S. B., Mason, K. O., Reichert, G. A., Warnock, A., & Kreidl, T. J. 1988, MNRAS, 233, 79
Howell, S. B., Mitchell, K. J., & Warnock, A. 1987, PASP, 99, 126
Irwin, J. B. 1952, ApJ, 116, 211
Marsh, T. R., Parsons, S. G., Bours, M. C. P., et al. 2014, MNRAS, 437, 475
Maxted, P. F. L., Napiwotzki, R., Dobbie, P. D., et al. 2006, Natur, 442, 543
Nogami, D., Kato, T., Baba, H., et al. 2001, MNRAS, 322, 79
Parsons, S. G., Marsh, T. R., Copperwheat, C. M., et al. 2010, MNRAS, 407, 2362
Patterson, J., Vanmunster, T., Skillman, D. R., et al. 2000, PASP, 112, 1584
Potter, S. B., Romero-Colmenero, E., Ramsay, G., et al. 2011, MNRAS, 416, 2202
Qian, S.-B., Han, Z.-T., Fernándes Lajús, E., et al. 2015, ApJS, 221, 17
Qian, S.-B., Han, Z.-T., Soonthornthum, B., et al. 2016, ApJ, 817, 151
Qian, S.-B., Liao, W.-P., Zhu, L.-Y., & Dai, Z.-B. 2010, ApJL, 708, L66
Qian, S.-B., Liu, L., Liao, W.-P., et al. 2011, MNRAS, 414, L16
Savoury, C., Littlefair, S., Dhillon, V., et al. 2011, MNRAS, 415, 2025
Szkody, P., & Howell, S. B. 1993, ApJ, 403, 743
Usher, P. D., Mattson, D., & Warnock, A. 1982, ApJS, 48, 51
Usher, P. D., Warnock, A., & Green, R. F. 1983, ApJ, 269, 73
Vaccaro, T. R., Wilson, R. E., Van Hamme, W., & Terrell, D. 2015, ApJ, 810, 157
Völschow, M., Banerjee, R., Hessman, F. V., et al. 2014, A&A, 562, A19
Völschow, M., Schleicher, D., Perdelwitz, V., & Banerjee, R. 2016, A&A, 587, A34
Warner, B. 1995, Cataclysmic Variable Stars Cambridge Astrophysics Series (Cambridge: Cambridge Univ. Press), 28
Wood, J. H., Irwin, M. J., & Pringle, J. E. 1985, MNRAS, 214, 475